LEPTON-FLAVOR VIOLATION IN SUPERSYMMETRIC MODELS WITH R-PARITY VIOLATION

KAZUHIRO TOBE

CERN, Theory Division, CH-1211 Geneva 23, Switzerland
E-mail: kazuhiro.tobe@cern.ch

Supersymmetric (SUSY) models with R-parity violation (RPV) can be an alternative scenario for non-zero neutrino masses. Within this framework, we discuss the lepton-flavor violating (LFV) processes $\mu \to e\gamma$, $\mu \to 3e$ and the $\mu \to e$ conversion in nuclei. We find the interesting features of LFV in RPV models, which are very different from other neutrino models such as SUSY models with heavy right-handed neutrinos. We show that a search for *all* the LFV processes is important to distinguish between the different models, and the measurement of P-odd asymmetries in polarized $\mu \to 3e$ is also useful to reveal the nature of LFV.

CERN-TH/2000-373 December 15 2000

1 Introduction

Recently, Super-Kamiokande experiments on atmospheric neutrinos have announced very convincing evidence for non-zero but tiny neutrino masses. In order to accommodate such small masses, new physics beyond the standard model (SM) is necessary. The most natural scenario to account for the tiny neutrino masses is the seesaw mechanism, where the small neutrino masses are a consequence of the presence of heavy right-handed neutrinos.

Within the framework of supersymmetric (SUSY) models, there is another possible scenario to accommodate non-zero neutrino masses, that is, SUSY models with R-parity violation (RPV), in which the lepton number is broken without heavy right-handed neutrinos being introduced. Therefore it is worthwhile to consider the low-energy consequences of this framework. Here we consider, particularly, the lepton-flavor violation (LFV) in muon processes such as $\mu \to e\gamma$, $\mu \to 3e$ and the $\mu \to e$ conversion in nuclei, since the most severe constraints on certain products of RPV couplings come from the current experimental bounds on these processes[1]. In this talk, we will see the general features of LFV in SUSY models with RPV, which are quite different from those in other neutrino mass models. We will stress that, in order to distinguish between the different models, all the LFV processes are important, and P-odd asymmetries in polarized $\mu \to 3e$ are also very useful to find the nature of LFV.

In the following sections, we discuss SUSY models with RPV and neutrino masses in this framework, and then consider LFV to see some of the general features in RPV models (for all details, see Ref.[2]).

2 SUSY models with R-parity violation

First let me remind you of the supersymmetric extension of the SM. As we listed in Table 1, the doublet lepton multiplet L has the same gauge quantum numbers as the Higgs multiplet H_d, whose vacuum expectation value (vev) induces the down-type and charged lepton mass terms. If we impose only standard model gauge symmetry (without R-parity) in the model, there is no reason to distinguish a lepton doublet from a Higgs. Thus in addition to the superpotential for the ordinary Yukawa couplings, we have the following superpotential:

$$W_{RPV} = \frac{\lambda_{ijk}}{2} L_i L_j \bar{E}_k + \lambda'_{ijk} L_i Q_j \bar{D}_k + \lambda''_{ijk} \bar{U}_i \bar{D}_j \bar{D}_k + \mu'_i L_i H_u, \qquad (1)$$

where the $LL\bar{E}$, $LQ\bar{D}$ and LH terms break the lepton number, and $\bar{U}\bar{D}\bar{D}$ breaks the baryon number; however, they are allowed by the SM gauge symmetry. We also have corresponding soft SUSY-breaking terms. However, the simultaneous existence of the couplings $LQ\bar{D}$ and $\bar{U}\bar{D}\bar{D}$ gives rise to rapid proton decay. The experimental limit from negative search for the proton decay provides very severe constraints on the R-parity couplings[1], for example $\lambda''_{11i}\lambda'_{11i} < 10^{-24}$ for $m_{\tilde{d}_i} = 1$ TeV. Thus we have to avoid such a rapid proton decay. One solution to the proton decay problem is "R-parity", which is the most popular solution in the SUSY SM. Doublet leptons and Higgs have different R-parity, as listed in Table 1, so that all terms in Eq. (1) are forbidden. The other solution is to impose the "baryon parity" or "lepton parity". If we require only baryon-parity conservation, the baryon-number violating term $\bar{U}\bar{D}\bar{D}$ is forbidden, and hence we can solve the proton decay problem. On the other hand, the lepton-number violating terms still exist. The existence of

Table 1. Gauge quantum numbers of lepton and Higgs multiplets in the minimal supersymmetric standard model

	$SU(3)_C$	$SU(2)_L$	$U(1)_Y$	R-parity
$\bar{E}$	1	1	1	−1
L	1	2	−1/2	−1
H_d	1	2	−1/2	+1
H_u	1	2	1/2	+1

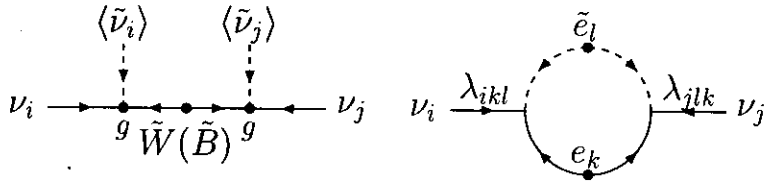

Figure 1. Feynman diagrams generating neutrino masses at tree level (left) and one-loop level (right).

such a lepton-number violation will be very interesting, since it can generate non-zero neutrino masses[1].

In the next section, we briefly discuss the neutrino masses within the framework of the RPV models to see that SUSY models with RPV can be an alternative scenario for the non-zero neutrino masses.

3 Neutrino masses in R-parity violating models

In models with RPV, sneutrinos and neutral Higgs can in general mix, because they have the same gauge quantum numbers. Thus sneutrinos also can have vevs. As a consequence, neutrino masses can be generated at tree level via a seesaw-type mechanism mediated by a Wino ($\tilde{W}$) and Bino ($\tilde{B}$), as shown in Fig. 1. Furthermore, the trilinear RPV couplings $LL\bar{E}$ and $LQ\bar{D}$ also generate the neutrino masses at the one-loop level. In Fig. 1, we show as an example the one-loop diagram which is induced by $LL\bar{E}$ couplings. Thus, very small but non-zero sneutrino vevs and RPV couplings can explain the non-zero neutrino masses. So far many works have been done and this framework is totally consistent with the non-zero neutrino masses[1]. The interesting point is that the RPV models can generate non-zero neutrino masses *without introducing heavy right-handed neutrinos*, and hence this is very different from the ordinary seesaw mechanism. Therefore the RPV models can be an alternative scenario to accommodate non-zero neutrino masses.

Now a question arising is "Can we distinguish between two different scenarios for neutrino masses?" To address this question, we will consider in the next section, in particular, the LFV in the charged lepton sector.

4 Lepton-flavor violation in muon processes

In SUSY models with heavy right-handed neutrinos (without RPV), event rates for LFV processes can be within the reach of near-future experiments, as discussed by Nomura[3] at this workshop. In this section, we discuss LFV in the framework of the RPV models.

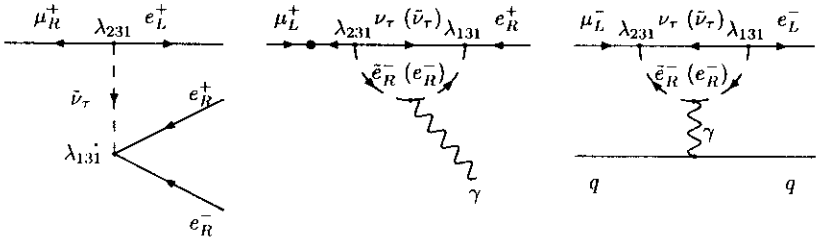

Figure 2. Feynman diagrams for LFV processes induced by $\lambda_{131}\lambda_{231}$.

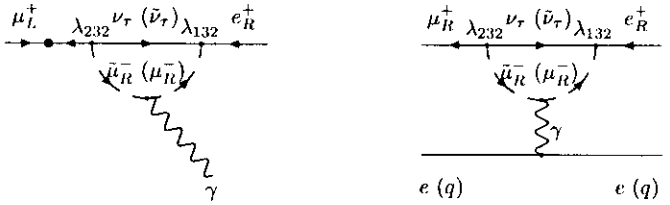

Figure 3. Feynman diagrams for LFV processes induced by $\lambda_{132}\lambda_{232}$.

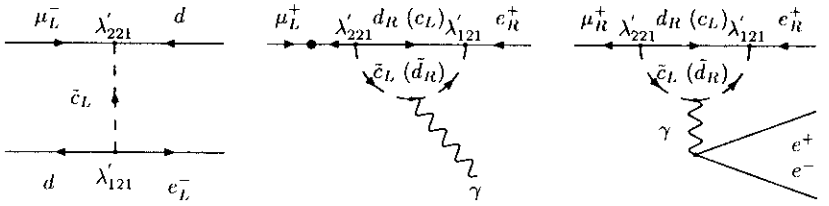

Figure 4. Feynman diagrams for LFV processes induced by $\lambda'_{121}\lambda'_{221}$.

In SUSY models with the RPV, the LFV in muon processes is induced by diagrams such as in Figs. 2–4. Here we only consider, for simplicity, the trilinear RPV terms $LL\bar{E}$ and $LQ\bar{D}$ in Eq. (1)[a].

First we show the constraints[1,2] on RPV couplings from LFV processes in Table 2, in which we assumed that only the listed pair of couplings is non-zero. The current upper limits on the branching ratios for LFV processes can put the most severe constraints on most of the listed couplings. Therefore, searches for LFV in muon processes are particularly sensitive to the RPV

[a] Even if the bilinear term $\mu' LH_u$ and the corresponding SUSY-breaking terms were non-zero, their contributions to LFV would be negligible because of neutrino mass constraints.

Table 2. Current (future) constraints on the R-parity violating couplings $LL\bar{E}$ and $LQ\bar{D}$ from LFV processes, assuming that only the listed pair of coupling is nonzero. The current (future) upper limits on the branching ratios are: $\mathrm{Br}(\mu \to e\gamma) < 1.2 \times 10^{-11}$ (10^{-14}), $\mathrm{Br}(\mu \to 3e) < 1.0 \times 10^{-12}$, and $\mathrm{R}(\mu \to e \text{ in Ti}) < 6.1 \times 10^{-13}$ ($\mathrm{R}(\mu \to e \text{ in Al}) < 10^{-16}$). Here we assume $m_{\tilde{\nu},\tilde{l}_R} = 100$ GeV and $m_{\tilde{q}} = 300$ GeV.

	$\mu \to e\gamma$	$\mu \to 3e$	$\mu \to e$ in nuclei
$\lvert\lambda_{131}\lambda_{231}\rvert$	2.3×10^{-4} (7×10^{-6})	6.7×10^{-7}	1.1×10^{-5} (2×10^{-7})
$\lvert\lambda_{132}\lambda_{232}\rvert$	2.3×10^{-4} (7×10^{-6})	7.1×10^{-5}	1.3×10^{-5} (2×10^{-7})
$\lvert\lambda_{133}\lambda_{233}\rvert$	2.3×10^{-4} (7×10^{-6})	1.2×10^{-4}	2.3×10^{-5} (4×10^{-7})
$\lvert\lambda_{121}\lambda_{122}\rvert$	8.2×10^{-5} (2×10^{-6})	6.7×10^{-7}	6.1×10^{-6} (1×10^{-7})
$\lvert\lambda_{131}\lambda_{132}\rvert$	8.2×10^{-5} (2×10^{-6})	6.7×10^{-7}	7.6×10^{-6} (1×10^{-7})
$\lvert\lambda_{231}\lambda_{232}\rvert$	8.2×10^{-5} (2×10^{-6})	4.5×10^{-5}	8.3×10^{-6} (1×10^{-7})
$\lvert\lambda'_{111}\lambda'_{211}\rvert$	6.8×10^{-4} (2×10^{-5})	1.3×10^{-4}	5.4×10^{-6} (2×10^{-7})
$\lvert\lambda'_{112}\lambda'_{212}\rvert$	6.8×10^{-4} (2×10^{-5})	1.4×10^{-4}	3.9×10^{-7} (7×10^{-9})
$\lvert\lambda'_{113}\lambda'_{213}\rvert$	6.8×10^{-4} (2×10^{-5})	1.6×10^{-4}	3.9×10^{-7} (7×10^{-9})
$\lvert\lambda'_{121}\lambda'_{221}\rvert$	6.8×10^{-4} (2×10^{-5})	2.0×10^{-4}	3.6×10^{-7} (6×10^{-9})
$\lvert\lambda'_{122}\lambda'_{222}\rvert$	6.8×10^{-4} (2×10^{-5})	2.3×10^{-4}	4.3×10^{-5} (7×10^{-7})
$\lvert\lambda'_{123}\lambda'_{223}\rvert$	6.9×10^{-4} (2×10^{-5})	2.9×10^{-4}	5.4×10^{-5} (9×10^{-7})

models. Furthermore, the future improvement of the limits on the event rates will be significant for the RPV models as shown in Table 2.

Even though results from neutrino and other experiments provide some constraints on the RPV couplings[1], it is difficult to make a definite prediction on the branching ratios for LFV processes since couplings which contribute to LFV processes are different from those which contribute to neutrino masses. Even in this framework, however, there are some interesting features of LFV, which are not only different from those in SUSY models with heavy right-handed neutrinos, but which can also be used to characterize the different cases themselves. To identify the features, we consider three representative cases[2] in next subsections.

4.1 Case (1): $\mu^+ \to e^+e^+e^-$ is induced at tree level

First, we consider a model in which only the Yukawa couplings λ_{131} and λ_{231} are non-zero. In this case, $\mu \to 3e$ is generated at tree level, while the other LFV processes ($\mu \to e\gamma$ and $\mu \to e$ conversion in nuclei) are induced via photon penguin diagrams at the one-loop level, as shown in Fig. 2. The ratios of branching ratios, $\mathrm{Br}(\mu \to e\gamma)/\mathrm{Br}(\mu \to 3e)$ and $\mathrm{R}(\mu \to e \text{ in nuclei})/\mathrm{Br}(\mu \to 3e)$ do not depend on the RPV couplings $\lambda_{131}\lambda_{231}$, so they are more predictive

quantities. For $m_{\tilde{\nu}_\tau} = m_{\tilde{e}_R} = 100$ GeV, we get

$$\frac{\mathrm{Br}(\mu \to e\gamma)}{\mathrm{Br}(\mu \to 3e)} = 1 \times 10^{-4}, \quad \frac{\mathrm{R}(\mu \to e \text{ in Ti (Al)})}{\mathrm{Br}(\mu \to 3e)} = 2\ (1) \times 10^{-3}. \qquad (2)$$

Since the $\mu \to 3e$ process is generated at tree level, its branching ratio is much larger than that of the other LFV processes. If such a scenario were realized in nature, the $\mu \to 3e$ process would be a discovery mode for the LFV in muon processes. In Table 3, we list results of other similar examples.

It is very important to emphasize that the ratios of branching ratios of the different processes are very different from those in SUSY models with heavy right-handed neutrinos (with R-parity conservation), which is different neutrino mass model. In SUSY models with heavy right-handed neutrinos, the following relations are approximately satisfied:

$$\frac{\mathrm{Br}(\mu \to e\gamma)}{\mathrm{Br}(\mu \to 3e)} = 1.6 \times 10^2, \quad \frac{\mathrm{R}(\mu \to e \text{ in Ti})}{\mathrm{Br}(\mu \to 3e)} = 0.92, \qquad (3)$$

since on-shell photon penguin diagram dominates over all others. Therefore, measurement of these ratios will be very important to distinguish between different neutrino mass models.

4.2 Case (2): all processes are induced at the one-loop level

Here we consider a different representative case, in which all of $\mu \to e\gamma$, $\mu \to 3e$ and $\mu \to e$ conversion in nuclei are induced at the one-loop level through the photon penguin diagram (Fig. 3). Suppose, as an example, that only the couplings λ_{132} and λ_{232} are non-zero. Then the ratios of branching ratios of the different processes are independent of the choice of $\lambda_{132}\lambda_{232}$:

$$\frac{\mathrm{Br}(\mu \to e\gamma)}{\mathrm{Br}(\mu \to 3e)} = 1.2, \quad \frac{\mathrm{R}(\mu \to e \text{ in Ti (Al)})}{\mathrm{Br}(\mu \to 3e)} = 18\ (11), \qquad (4)$$

for $m_{\tilde{\nu}_\tau} = m_{\tilde{\mu}_R} = 100$ GeV. Because of the log-enhancement of the off-shell photon penguin diagram, the event rates for $\mu \to 3e$ and $\mu \to e$ conversion in nuclei can be as large as the branching ratio for the $\mu \to e\gamma$ process, even though they are higher-order processes in QED. We also show the dependence on the slepton masses of these ratios of branching ratios in Fig. 5. All the LFV processes are equally relevant in most of the parameter space. Again we stress that these ratios of the branching ratios are very different in SUSY models with heavy right-handed neutrinos [see Eq. (3)].

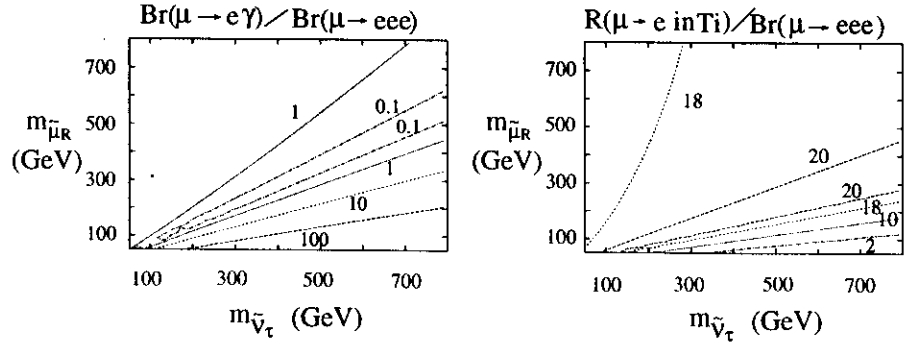

Figure 5. Contours of constant $B_{e\gamma}/B_{3e}$ (left), and $R_{conv.}/B_{3e}$ (right) in the ($m_{\tilde{\mu}_R} \times m_{\tilde{\nu}_\tau}$) plane, assuming that only the product of $LL\bar{E}$ couplings $\lambda_{132}\lambda_{232}$ is non-zero.

4.3 Case (3): $\mu^- \to e^-$ conversion at tree level

Here, we consider the possibility that $\mu \to e$ conversion in nuclei is induced at tree level. This can arise through some of the $\lambda' LQ\bar{D}$ terms. As an example, we consider a model in which only λ'_{121} and λ'_{221} are non-zero, so that $\mu \to e$ conversion is induced at tree level, while $\mu \to e\gamma$ and $\mu \to 3e$ are generated at one-loop level (Fig. 4). In this case, ratios of branching ratios are given by

$$\frac{\mathrm{Br}(\mu \to e\gamma)}{\mathrm{Br}(\mu \to 3e)} = 1.1, \quad \frac{\mathrm{R}(\mu \to e \text{ in Ti (Al)})}{\mathrm{Br}(\mu \to 3e)} = 2\ (1) \times 10^5, \tag{5}$$

where we assume $m_{\tilde{d}_R} = m_{\tilde{c}_L} = 300$ GeV. Since $\mu \to e$ conversion is induced at tree level, its event rate is much larger than that of other processes, as expected. In $\mu \to 3e$, the off-shell photon penguin vertex dominates over the other contributions because of the log-enhancement. Therefore, the ratio of branching ratios $\mathrm{Br}(\mu \to e\gamma)/\mathrm{Br}(\mu \to 3e)$ is very similar to that we obtained in the previous subsection. Results of other similar examples are also listed in Table 3.

4.4 P-odd asymmetries in polarized $\mu^+ \to e^+e^+e^-$ process

When the muon is polarized in $\mu \to 3e$ process, two P-odd asymmetries (A_{P_1} and A_{P_2}) can be defined[4]. Following the notation introduced by Okada *et al.*[4], here we only show the results in Table 3. For details, see Ref.[2]. As can be seen from the table, the measurement of these P-odd asymmetries is useful to distinguish the three different representative cases in RPV models, and also important to clearly separate the different neutrino models.

Table 3. The ratios of branching ratios $\mathrm{Br}(\mu \to e\gamma)/\mathrm{Br}(\mu \to 3e)$ and $\mathrm{R}(\mu \to e \text{ in Ti})/\mathrm{Br}(\mu \to 3e)$, A_{P_1} and A_{P_2} for $\mu \to 3e$ are shown when the listed pair of Yukawa couplings is dominant. Here, we assume $m_{\tilde{\nu},\tilde{l}_R} = 100$ GeV and $m_{\tilde{q}} = 300$ GeV. We also show a typical result obtained for SUSY models with heavy right-handed neutrinos and R-parity conservation.

		$\frac{\mathrm{B}_{e\gamma}}{\mathrm{B}_{3e}}$	$\frac{\mathrm{R}_{\mathrm{conv.}}}{\mathrm{B}_{3e}}$	A_{P_1}	A_{P_2}	$\frac{A_{P_1}}{A_{P_2}}$
Case (1)	$\lambda_{131}\lambda_{231}$	1×10^{-4}	2×10^{-3}	+19%	−15%	−1.3
	$\lambda_{121}\lambda_{122}$	8×10^{-4}	7×10^{-3}	−19%	+15%	−1.3
	$\lambda_{131}\lambda_{132}$	8×10^{-4}	5×10^{-3}	−19%	+15%	−1.3
Case (2)	$\lambda_{132}\lambda_{232}$	1.2	18	−25%	−5%	5.6
	$\lambda_{133}\lambda_{233}$	3.7	18	−25%	−4%	6.2
	$\lambda_{231}\lambda_{232}$	3.6	18	+25%	+4%	6.2
	$\lambda'_{122}\lambda'_{222}$	1.4	18	−25%	−4%	5.7
	$\lambda'_{123}\lambda'_{223}$	2.2	18	−25%	−4%	5.9
Case (3)	$\lambda'_{111}\lambda'_{211}$	0.4	3×10^2	−26%	−5%	5.4
	$\lambda'_{112}\lambda'_{212}$	0.5	8×10^4	−26%	−5%	5.4
	$\lambda'_{113}\lambda'_{213}$	0.7	1×10^5	−26%	−5%	5.5
	$\lambda'_{121}\lambda'_{221}$	1.1	2×10^5	−26%	−5%	5.6
MSSM with ν_R		1.6×10^2	0.92	10%	17%	0.6

5 Conclusions

We discussed the LFV of muon processes in SUSY models with RPV. Interestingly the general features of LFV are very distinct from those of SUSY models with heavy right-handed neutrinos and R-parity conservation. *All* the LFV processes can be very important to distinguish between different models. Future experimental improvement of all the LFV limits will be significant to reveal the nature of LFV and the origin of neutrino masses.

Acknowledgments

The author would like to thank the organizers for a very interesting Workshop.

References

1. For a recent review on RPV, see H. Dreiner, in *Perspectives on Supersymmetry*, ed. G.L. Kane (World Scientific, Singapore, 1998). See also Ref.[2] for a complete set of references.

2. A. de Gouvêa *et al.*, hep-ph/0008085, to appear in *Phys. Rev.* **D**.
3. See D. Nomura, contribution to this workshop.
4. Y. Okada *et al.*, *Phys. Rev.* D **58**, 051901 (1998); **61**, 094001 (2000). See also Y. Okada, contribution to this workshop.